Available online at www.sciencedirect.com
SCIENCE DIRECT®
Journal of Power Sources 127 (2004) 162–171
JOURNAL OF POWER SOURCES
www.elsevier.com/locate/jpowsour

Dependence of PEM fuel cell performance on catalyst loading

H.A. Gasteiger*, J.E. Panels, S.G. Yan
General Motors, Fuel Cell Activities, Honeoye Falls, NY 14472, USA

Abstract

This study focuses on a determination of the cell voltage losses observed for Pt and PtRu loading reductions in H_2/air and reformate/air polymer/electrolyte-membrane fuel cells (PEMFC). Experiments with catalyst-coated membranes (CCM) of varying anode and cathode catalyst loadings with H_2/O_2 and H_2/air demonstrate that the anode catalyst loading in *state-of-the-art* membrane electrode assemblies (MEAs) operating on pure H_2 can be reduced to 0.05 mg_{Pt}/cm^2 without significant voltage losses, while the cell voltage losses upon a reduction of the cathode catalyst loading from 0.40 to 0.20 mg_{Pt}/cm^2 for optimized MEAs amounts to 10–20 mV, consistent with purely kinetic losses due to the oxygen reduction reaction. It is shown that H_2/air operation with *state-of-the-art* MEAs very closely approaches the Pt-specific power density (in units of g_{Pt}/kW) for large-scale automotive fuel cell applications with pure H_2 feed.

For reformate/air operation, PtRu anode loadings can be reduced to 0.20 mg_{PtRu}/cm^2 for reformate containing 100 ppm CO with a 2% air-bleed. Any further reduction will, however, require either a change in operating conditions (i.e. lower CO concentration or cell temperature $\gg$80 °C) or novel, more CO-tolerant anode catalysts.

Keywords: Platinum loading; Polymerelectrolyte membrane (PEM) fuel cell; Platinum–ruthenium; Oxygen reduction reaction activity; CO-tolerance

1. Introduction

Over the past two decades, extensive research on the development of low-temperature polymerelectrolyte-membrane fuel cells (PEMFC) resulted in significant increases in the voltage performance of membrane electrode assemblies (MEAs) [1]. These voltage gains were primarily produced by the implementation of thinner membranes, progressing from the originally most common 1100 EW (equivalent weight ($g_{polymer}/mol_{H^+}$)) Nafion® membranes with thickness of 175 μm/125 μm (Nafion 117/115) [2,3], to 50 μm thick Nafion® 112 [4], all the way to ultra-thin homogeneous (e.g. 25 μm, 1100 EW membranes extruded in the sulfonylfluoride-form from DuPont and hydrolyzed to proton-form by Ion Power (USA) [5]) or lower-EW PTFE/ionomer composite membranes (either from Asahi Glass (30 μm, 910 EW [6]) or Gore (25 μm, <1000 EW [7])) which produce high cell voltages at current densities ≥1 A/cm^2. These cell voltage improvements were accompanied by significant reductions in MEA platinum loadings from the high loadings of 5–10 mg_{Pt}/cm^2 per MEA in the early 1990s [8] to <1 mg_{Pt}/cm^2 per MEA in later work [4,9], a development which was primarily due to the substitution of Pt-black catalysts with higher surface area carbon-supported Pt catalysts as well as the use of perfluorosulfonic-ionomer binder in thin-film catalyst layers [1,10].

Due to these innovations in materials and processing technology, *state-of-the-art* fuel cells yield cell voltages which surpass older MEA technology, where only up to 0.60 V were achieved at 1.0 A/cm^2 under high pressure conditions (300 kPa_{abs}) with fully humidified H_2/air reactants (stoichiometric flows of 1.5/2.0) at cell temperatures of 70–80 °C and Pt loadings of <1 mg_{Pt}/cm^2 per MEA [3]. This is, for example, illustrated by reports from UTC Fuel Cells, where 0.68 V are obtained at the same current density (1.0 A/cm^2) even at ambient pressure under otherwise similar conditions (65 °C cell temperature, fully humidified H_2/air at stoichiometric flows of 1.25/2.0) [11,12]. In the latter case, rather low Pt cathode loadings of 0.4 mg_{Pt}/cm^2 were used [11] and Pt loadings on the anode were probably of the same value or lower (not cited). While this represents a major development progress, the Pt-specific power density still equates to ca. 0.9–1.2 g_{Pt}/kW (assuming anode Pt loadings of 0.2–0.4 mg_{Pt}/cm^2, i.e. total loadings of 0.6–0.8 mg_{Pt}/cm^2 per MEA), which may be sufficiently low for low-volume applications (e.g. stationary, uninterrupted-power supply, etc.), but is still too high for automotive applications, where less than 0.4 g_{Pt}/kW are required for large-scale implementation [13].

Primarily two approaches may be used to reduce the Pt metal requirement in *state-of-the-art* fuel cells: (i) reduction

* Corresponding author.
E-mail address: hubert.gasteiger@gm.com (H.A. Gasteiger).

0378-7753/$ – see front matter © 2004 Elsevier B.V. All rights reserved.
doi:10.1016/j.jpowsour.2003.09.013

of the mass-transport losses particularly at high current densities by improved diffusion media (DM), improved reactant flow-fields, and improved electrode structures and/or (ii) improved catalysts and catalyst utilization. The former approach would allow to increase the stack current density to 1.5–2.0 A/cm^2 with no or insignificant voltage penalty [5], thereby reducing the Pt-specific power density by a factor of 1.5–2 (i.e. 0.45–0.6 g_{Pt}/kW). Any further reductions would have to be achieved by a reduction of the Pt loading of the MEA below the above 0.6–0.8 mg_{Pt}/cm^2 per MEA, which may either be done via platinum thrifting or the implementation of alternative catalysts (e.g. Pt-alloy cathode catalysts [2,14]).

The present work examines in detail the effect of platinum loading reductions (both anode and cathode) on fuel cell performance and seeks to demonstrate the trade-off between Pt-catalyst loading and cell voltage. This will be illustrated by means of 50 cm^2 single-cell data complemented by full-active-area short stack (250 and 500 cm^2 active-area, ca. 20 cells) measurements. Owing to the high catalytic activity of Pt toward H_2 electro-oxidation (exchange-current densities, i_0, of the order of 10^{-3} A/cm$^2_{Pt}$ [15]), we will show that there is a large potential for reducing Pt anode loadings in the case of fuel cell operation with pure H_2, while much less reductions are achievable with current PtRu-anode catalysts in the case of fuel cell operation with CO-contaminated reformate. Unfortunately, the oxygen reduction reaction (ORR) kinetics on Pt are approximately six orders of magnitude slower than the H_2 oxidation kinetics (i_0 of the order of 10^{-9} A/cm$^2_{Pt}$ [5]), and we will show that further reductions in cathode Pt loadings with pure Pt-catalysts result in well predictable voltage losses (these may, however, be avoided by implementing more advanced Pt-alloy cathode catalysts [2,14]).

2. Experimental procedure

2.1. MEA preparation

All catalyst-coated membranes (CCM) for both small-scale (50 cm^2) and short-stack testing (250 and 500 cm^2) were prepared in-house by an identical procedure [5]. Carbon-supported 47 wt.% Pt/carbon (Tanaka, Japan) and 57 wt.% $Pt_{0.33}Ru_{0.66}$/carbon (Tanaka, Japan) as well as organic ionomer solutions (either 5 wt.% Nafion® with 1100 EW (DuPont) or a different ca. 900 EW ionomer solution) were used to fabricate thin-layer electrodes which were transferred via a decal method onto either extruded Nafion® 112 (50 μm thickness, 1100 EW; DuPont) or a ca. 25 μm low-EW membrane (ca. 900 EW). An ionomer/carbon ratio of approximately 0.8/1 (weight ratio) was maintained in the electrodes of all prepared CCMs using ionomers identical to the ones used in the membrane. CCMs with various catalyst loadings were produced for this study and loadings are referred to as anode-loading/cathode-loading (e.g. 0.2/0.4 mg_{Pt}/cm^2 refers to a 0.2 mg_{Pt}/cm^2 anode and a 0.4 mg_{Pt}/cm^2 cathode loading).

Gas-diffusion media were treated in-house and are based on carbon fiber paper substrates (Toray Inc., Japan). Both anode and cathode DMs were teflonated and additionally processed using a proprietary surface treatment. Single cells (50 cm^2 active-area) and ca. 20 cell short stacks (250 and 500 cm^2 active-area) were assembled by sandwiching CCMs between the appropriate DMs and applying an average compressive load of approximately 1500 kPa_{abs} to the active-area.

2.2. Determination of H_2 cross-over

Due to the low but finite solubility and diffusivity of H_2 in the ionomer [1], H_2 permeates from the anode compartment of a PEMFC to the cathode, where it is oxidized electrochemically in the typical cathode potential (0.5–1.0 V versus RHE, depending on the current density). The resulting parasitic H_2 oxidation current density is generally referred to as H_2-cross-over current density, i_x, and can be determined experimentally using the so-called driven-cell mode, by polarizing the N_2-purged cathode compartment at >(+0.4) V with respect to the H_2-purged anode compartment. (At >(+0.4) V, the resulting H_2 oxidation current density is purely limited by the H_2 permeation rate.) This method is described in detail in [11] where it is also shown that the observed H_2-cross-over current density increases with increasing H_2 partial pressure and increasing cell temperature. For this study, we experimentally evaluated the H_2-cross-over current densities for Nafion™ 112-based MEAs under fully humidified conditions at 270 kPa_{abs} and 80 °C (i.e. p_{H_2} = 223 kPa_{abs}), yielding a value of 3.3 mA/cm^2. It may be noted that this value, used in the kinetic analysis of our experimental data, is ca. 35% lower than the value reported in [11], reflecting the large experimental error in the evaluation of the H_2 permeation rate.

2.3. Fuel cell testing

Fuel cell stations from Fuel Cell Technology (Los Alamos, NM) were used to test 50 cm^2 active-area MEAs. Pure oxygen or air were used as cathode reactants and pure H_2 as anode reactant (all gases of 99.99% purity). Generally, stoichiometric flow rates were used in all experiments except in those where it is noted explicitly in the figure captions. Reactant humidification was achieved by water-bubblers, the temperature of which was calibrated to yield the quoted relative humidity (RH) values. Cell resistances as a function of current density (i.e. the sum of the proton-conduction resistance in the membrane and the various electronic resistances (bulk and contact resistances)) were determined using an ac perturbation of 1 kHz. For each data point, the cell voltage was stabilized over 15 min and data were averaged over the last 5 min. Multiple-path serpentine flow-fields (two and three parallel channels for

the anode and cathode, respectively) machined into sealed graphite blocks (Poco) were used for 50 cm^2 testing. The flow-field channel width was approximately 0.8 mm with a channel/land width ratio of 1.3/1.

For short-stack testing (ca. 20 cells each), 250 and 500 cm^2 active-area MEAs with different catalyst loadings and membranes were tested in the same stack. Performance data shown in each figure in this work represent the average of four nominally identical samples in the same short-stack. Cell resistances in the short-stack were measured the same way as in the above described 50 cm^2 testing. The flow-field configuration of the short-stack is proprietary; for short stack testing hydrogenics teststands were used.

3. Results

3.1. Effect of anode Pt loadings for pure H_2 fuel

As was mentioned in Section 1, the H_2 oxidation reaction (HOR) kinetics on platinum are very facile, characterized by exchange-current densities of the order of 10^{-3} A/cm^2_{Pt} [15]. As a matter of fact, the HOR kinetics are so fast that it becomes very difficult to experimentally determine i_0's and Tafel-slopes due to the interference from mass-transport resistances in most experimental set-ups. One recent attempt to determine the HOR and hydrogen evolution reaction (HER) kinetics was published by Markovic et al. [15], using platinum single-crystal electrodes in a rotating-disk electrode (RDE) configuration in 0.05 M H_2SO_4 at 60 °C with pure H_2 at atmospheric pressure (100 kPa). The highest exchange-current density amongst the low-index Pt single-crystals was obtained for Pt(1 1 0) with a value of 1.35 mA/cm^2_{Pt} and a Tafel-slope of 33 mV per decade. Using these kinetic parameters, one may estimate the anode overpotential as a function of current density and platinum loading in an operating fuel cell at similar H_2 partial pressures and similar temperatures using the Buttler–Volmer equation:

$$i = i_{0(60\,^\circ\mathrm{C},100\,\mathrm{kPa\,H_2})}\,\mathrm{rf}\,(10^{(E_{\mathrm{anode}}-E_{\mathrm{eq.}})/\mathrm{TS}} - 10^{(E_{\mathrm{eq.}}-E_{\mathrm{anode}})/\mathrm{TS}}) \quad (1)$$

where rf is the roughness factor of the electrode in units of cm^2_{Pt}/cm^2 (note that cm^2 refers to the geometric surface area of the electrode of an MEA throughout this study), TS the Tafel-slope, and E_{anode} the anode potential with respect to the reversible H_2 potential $E_{eq.}$ ($E_{eq.} = 0$ V).

Electrodes prepared in this study have an electrochemically accessible Pt surface area of 52 m^2/g_{Pt} (ca. 90% Pt-catalyst utilization), resulting in roughness factors of 210 and 26 cm^2_{Pt}/cm^2 for Pt loadings of 0.40 and 0.05 mg_{Pt}/cm^2, respectively [5]. Fig. 1 shows the calculated anode

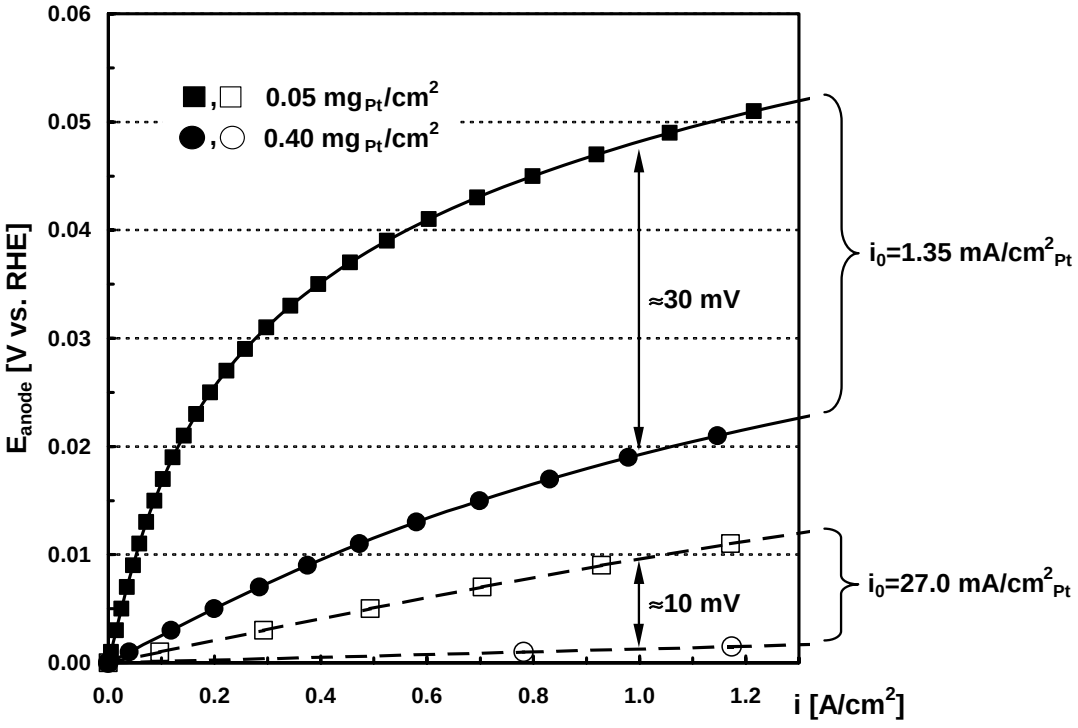

Fig. 1. Anode overpotentials as a function of current density and Pt loading calculated from Eq. (1) using roughness factors (rf) of 210 and 26 cm^2_{Pt}/cm^2 for anode catalyst loadings of 0.40 and 0.05 mg_{Pt}/cm^2, respectively. Solid lines and symbols refer to values calculated from the exchange-current density ($i_0 = 1.35$ mA/cm^2_{Pt}) and Tafel-slope (TS = 33 mV per decade) reported by Markovic et al. [15] for Pt(1 1 0) in 0.05 M H_2SO_4 at 60 °C and 100 kPa H_2. Dashed lines and open symbols refer to calculations based on at 20-fold larger value for the exchange-current density ($i_0 = 27.0$ mA/cm^2_{Pt}) but using the same Tafel-slope.

overpotentials as a function of current density for these two different loadings, using Eq. (1) and the above reported kinetic parameters (solid lines and symbols). Based on these calculations and under comparable experimental conditions (i.e. 100 kPa H_2 partial pressure and ca. 60 °C), MEAs with an anode loading of 0.05 mg_{Pt}/cm^2 would be expected to yield ca. 30 mV lower cell voltages at 1.0 A/cm^2 compared to MEAs with a higher anode loading of 0.40 mg_{Pt}/cm^2. As the reported activation energy for the HOR/HER kinetics of 9.5 kJ/mol is very low [15], small changes in temperature are not significantly changing this prediction.

Fig. 2 shows the change in the H_2/air 50 cm^2 single-cell performance as the anode loading is being reduced from 0.40 to 0.10 and 0.05 mg_{Pt}/cm^2, recorded at 80 °C under fully humidified conditions at a total pressure of 150 kPa_{abs} (note that the H_2 partial pressure is actually 100 kPa since the water vapor pressure is ca. 50 kPa under these conditions). Quite obviously, the differences in cell voltage are only of the order of 10 mV and do not reflect the above predicted differences of 30 mV. This can also be seen more clearly in Fig. 3, where the cell voltage difference, ΔE_{cell}, between the lower-loaded anodes and the 0.40 mg_{Pt}/cm^2 anode are plotted versus current density. It is difficult to rationalize this discrepancy by postulating mass-transport resistances in the thicker higher-loaded electrode (ca. 13 μm for 0.40 mg_{Pt}/cm^2 [5] and ca. 2 μm for 0.05 mg_{Pt}/cm^2), since the kinetic model in Fig. 1 predicts already 20 mV kinetic losses at current densities as low as 0.2 A/cm^2 where mass-transport on the anode side should be negligible. The only alternative explanation is that the "true" exchange-current density for the HOR/HER is significantly larger than the value reported by Markovic et al. [15], and a 20-fold larger i_0 would yield quantitative agreement between the kinetic model (dashed lines and open symbols in Fig. 1) and the experimental data in Figs. 2 and 3.

Short-stack testing of scaled-up versions (250 cm^2) of the MEAs used for the experiments in Figs. 2 and 3 under the same conditions except for reduced cathode–air humidification (64 °C dewpoint, corresponding to 50% RH) was conducted subsequently to confirm the above observations. This is shown in Fig. 4, where the error bars represent the standard deviation between four replicates for each loading (i.e. $\sigma^2_{\text{difference}} = (\sigma^2_{0.4\,mg_{Pt}/cm^2} + \sigma^2_{x\,mg_{Pt}/cm^2})^{0.5}$) in a ca. 20-cell short-stack. In this case, the observed differences are somewhat larger than what was observed in Fig. 3, but still lower than the prediction of the kinetic model with the reported exchange-current density of 1.35 mA/cm^2_{Pt} (solid lines and symbols in Fig. 3). This discrepancy between the 50 and 250 cm^2 MEA testing was subsequently found to be due to non-optimized MEA scale-up and recent measurements (not shown here) indeed confirmed the conclusions drawn from Figs. 2 and 3, namely that an anode loading reduction from 0.40 to 0.05 mg_{Pt}/cm^2 results in voltage losses of less than 10 mV at current densities up 1.0 A/cm^2.

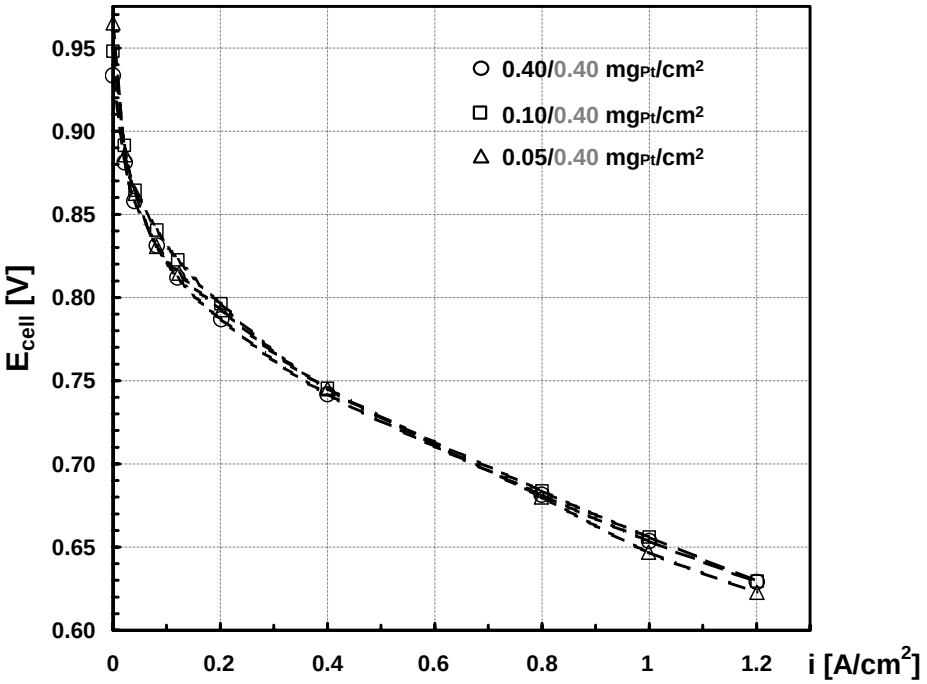

Fig. 2. Effect of anode Pt loading on 50 cm^2 single cell voltage, E_{cell}, for H_2/air operation at 80 °C and 150 kPa_{abs} with fully humidified reactants (80 °C dewpoints) at stoichiometric H_2/air flows of $s = 2.0/2.0$ for $i \geq 0.2$ A/cm^2 (at $i < 0.2$ A/cm^2, H_2/air-flow rates remained constant at 0.2 A/cm^2 flows). Anode loadings varied from 0.40 to 0.05 mg_{Pt}/cm^2 while all cathode loadings were 0.40 mg_{Pt}/cm^2. Catalyst-coated membranes were prepared in-house using ca. 25 μm thick/900 EW membranes and ca. 900 EW ionomers in the electrode, and 47 wt.% Pt/carbon catalysts. Voltages were averaged between 10 and 15 min holding time at each current density.

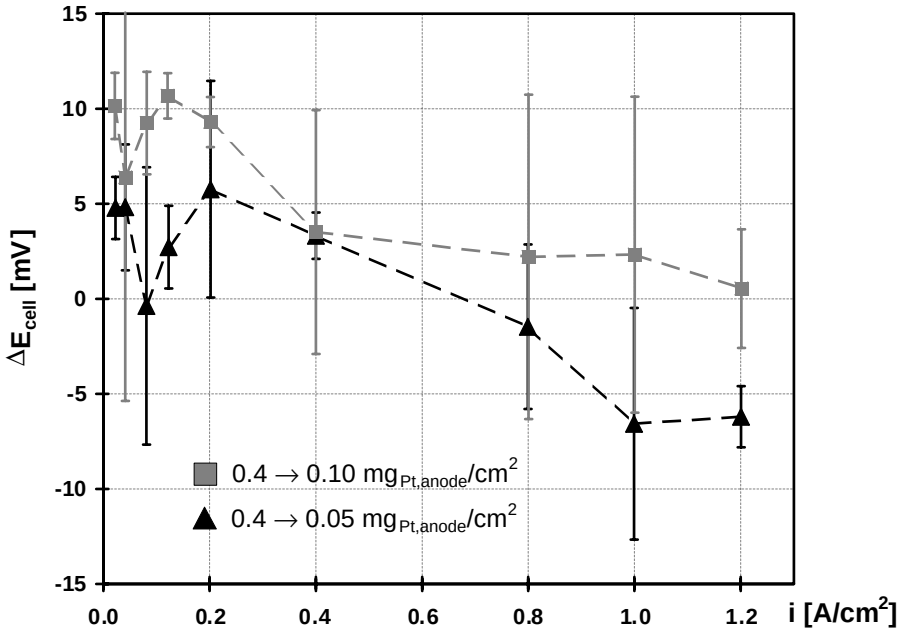

Fig. 3. Cell voltage differences, ΔE_{cell}, between MEAs with reduced anode loadings and the MEA with the highest anode loading of 0.40 mg_{Pt}/cm^2. Data were extracted from Fig. 2. Positive *y*-axis values indicate performance better than that of the reference-loading MEA (i.e. 0.40/0.40 mg_{Pt}/cm^2).

In conclusion, anode loadings as low as 0.05 mg_{Pt}/cm^2 (and maybe even lower) are possible without significant cell voltage losses for fuel cell operation with pure H_2. Considering a cell voltage of 0.65 V at 1.0 A/cm^2 shown in Fig. 2, this translates into a Pt-specific power density of the anode electrode of 0.08 g_{Pt}/kW with Nafion® 112 based MEAs. Even lower values are achieved with thinner membranes and lower-EW ionomers for which higher cell voltages can be

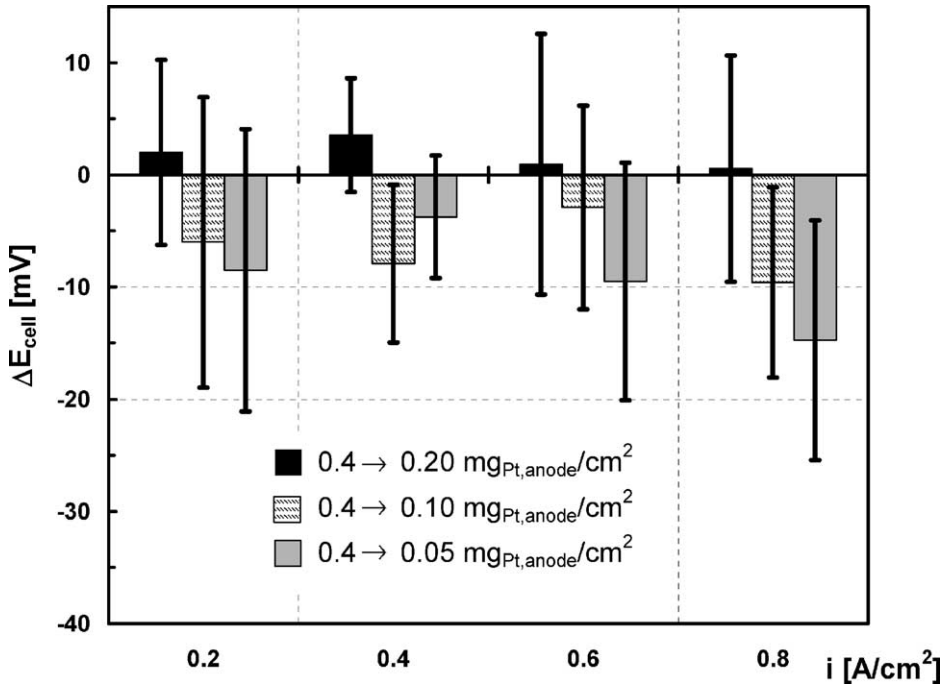

Fig. 4. Cell voltage differences, ΔE_{cell}, between 250 cm^2 active-area MEAs with reduced anode loadings referenced to MEAs with anode loadings of 0.40 mg_{Pt}/cm^2 (all cathode loadings are 0.40 mg_{Pt}/cm^2). Positive *y*-axis values indicate improved performance compared to the reference-loading MEAs (i.e. 0.40/0.40 mg_{Pt}/cm^2). MEAs were tested in a short-stack (four replicate MEAs for each loading) at 80 °C and 150 kPa_{abs} with partially humidified H_2/air (80/64 °C dewpoints anode/cathode) at stoichiometric flows of $s = 1.3/2.0$ (H_2/air). Catalyst-coated membranes with 250 cm^2 active-area were prepared according to the same procedure and using the same components as the 50 cm^2 catalyst-coated membranes described in Fig. 2. Voltages were averaged between 10 and 15 min holding time at each current density.

obtained due to reduced membrane resistance and improved water-management [5]. Therefore, *state-of-the-art* Pt anode loadings are already quite acceptable for large-scale automotive fuel cell applications with pure H_2 fuel.

3.2. Effect of anode PtRu loadings for reformate fuel

H_2-rich reformate derived from steam-reforming or partial-oxidation of hydrocarbons with subsequent water–gas-shift and preferential-CO-oxidation clean-up is generally contaminated with 10–100 ppm CO which strongly poisons the HOR on conventional Pt-catalysts. Early studies in 1967 already determined that PtRu catalysts show a significantly enhanced CO-tolerance over Pt [16], where CO-tolerance is defined as the voltage loss, η_{CO}, between fuel cell operation with dilute H_2 and CO-contaminated reformate with the same H_2 concentration (i.e. voltage losses in the absence of H_2-dilution effects). In order to minimize η_{CO} for reasonably low anode loadings ($\leq$1 mg_{PtRu}/cm^2), an air-bleed into the reformate feed-stream is generally required [17]. Typical air-bleed levels with reformate feed and *state-of-the-art* MEAs (0.5–0.4 mg_{PtRu}/cm^2) are 2–3% (vol.% referenced to the total reformate stream) for 40 [18] and 50 ppm CO [19] and up to 5% for 500 ppm CO [20].

Fig. 5 shows the CO-induced voltage loss, η_{CO}, for gasoline-reformate (40% H_2, 20% CO_2, balance N_2) with 100 ppm CO and 2% air-bleed for *state-of-the-art* PtRu loadings of 0.40 mg_{PtRu}/cm^2 as a function of current density at typical operating conditions (80 °C cell temperature, 80/64 °C dewpoints, and stoichiometrich reformate/air flows of 1.3/2.0 at 150 kPa_{abs}). Under these conditions, no CO-induced voltage loss can be observed, consistent with the above literature reports. However, analogous to the observation with Pt anodes [21,22], the CO-tolerance at any given CO concentration (and, by extension, at any given air-bleed level) does depend on the mass-specific current density (i.e. the ratio of current density and metal loading in units of (A/mg_{Pt}) or (A/mg_{PtRu})) so that a reduction in noble-metal loading will finally lead to an increase in η_{CO}, particularly at increasing current densities. Under the conditions of Fig. 5, this does not yet occur as the PtRu loading is reduced to 0.20 mg_{PtRu}/cm^2, but CO-induced voltage losses become unacceptably large for the lower loading of 0.10 mg_{PtRu}/cm^2, particularly at higher current densities. Significantly higher air-bleed levels (>4%) would again diminish these losses for the 0.10 mg_{PtRu}/cm^2 anode, but are not acceptable based on overall system efficiency and operation.

In conclusion, 0.2 mg_{PtRu}/cm^2 is the minimum loading which can be practically achieved with *state-of-the-art* PtRu catalysts for reformate operation with 100 ppm CO. Lower loadings could only be achieved by significantly reduced CO concentrations, higher operating temperatures, or the development of novel CO- and CO_2-tolerant anode catalysts (e.g.

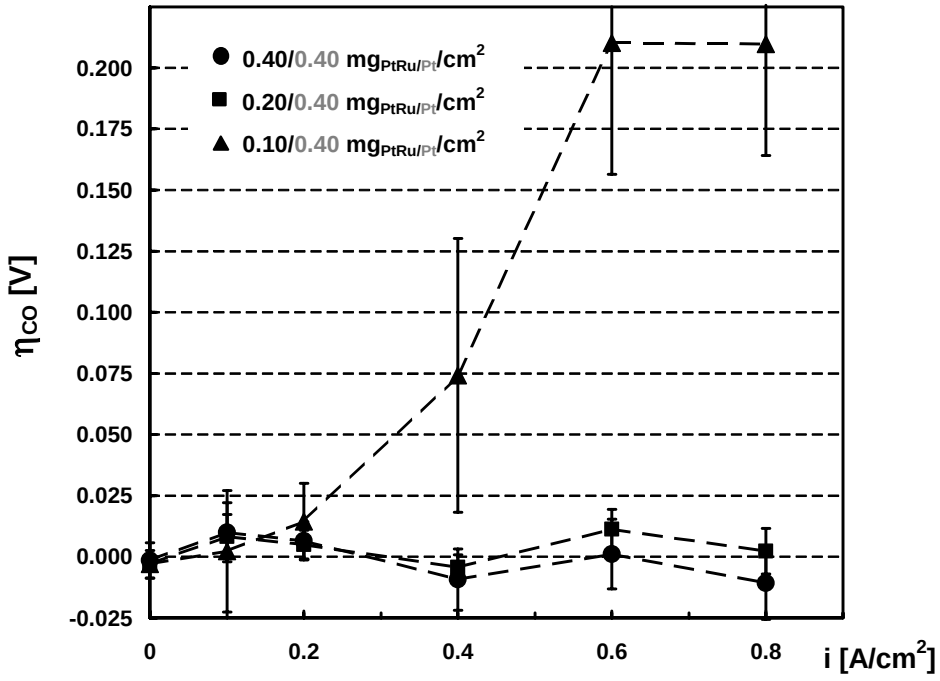

Fig. 5. CO-induced overpotentials as a function of current density for MEAs with varying PtRu anode loadings (all cathode loadings are 0.40 mg_{Pt}/cm^2). Cell voltages were obtained from 500 cm^2 active-area short-stack measurements (four replicate MEAs for each loading) with 40% H_2 reformate (20% CO_2, balance N_2) containing 100 ppm CO in the presence of 2% air-bleed and referenced to cell voltages obtained for operation with CO-free dilute 40% H_2 reactant (balance N_2). Test conditions: 80 C, 150 kPa_{abs}, and reactant dewpoints of 80/64 °C (fuel/air) at stoichiometric flows of 1.3/2.0 (fuel/air). Catalyst-coated membranes with 500 cm^2 active-area were prepared according to the same procedure as the 50 cm^2 catalyst-coated membranes described in Fig. 2. Voltages were averaged between 10 and 15 min holding time at each current density.

PtMo catalysts do have superior CO-tolerance but cannot be used in the presence of high CO_2 concentrations due to the reverse water-gas-shift reaction [18]). Therefore, the achievable Pt-specific power densities of PtRu anode electrodes in reformate operation are atleast a factor of four larger (>0.3 g_{PtRu}/kW) than what can already be obtained for Pt anodes in pure H_2 operation and further R&D on CO-tolerant catalysts is required to achieve automotive Pt-metal-specific power densities of <0.4 $g_{Pt\text{-}metal}$/kW (sum of anode and cathode).

3.3. Effect of cathode Pt loadings for H_2/air operation

3.3.1. Oxygen reduction kinetics in PEFCs determined by H_2/O_2 50 cm^2 testing

To evaluate the impact of the oxygen reduction reaction kinetics on PEFC performance, catalyst-coated Nafion® 112 membranes (N112) with variable Pt cathode loadings were tested with fully humidified H_2/O_2 reactants at 270 kPa_{abs} and a cell temperature of 80 °C. For a quantitative assessment of the impact of the ORR kinetics on PEFC performance, it is most straightforward to examine the resistance-corrected cell voltages, $E_{iR\text{-free}}$:

$$E_{iR\text{-free}} = E_{\text{cell}} + iR_{\Omega} \tag{2}$$

where the R_{Ω} term in Eq. (2) refers to the sum of ohmic resistance contributions produced by both electronic (DM/flow-field and DM/catalyst-layer contact-resistances as well as bulk resistances in the DM and the catalyst-layer) and protonic (H^+ conduction in the membrane) resistance losses. By correcting the raw voltage data with experimentally determined values of R_{Ω} (see Section 2), the effect of possibly varying ohmic resistances with varying Pt cathode loadings can be eliminated from the independent effect of Pt cathode loading on the PEFC performance.

Fig. 6a shows the resistance-corrected cell voltages versus the H_2-cross-over-corrected current density ($i_{\text{eff}} = i + i_x$, $i_x = 3.3\,\text{mA/cm}^2$) for 50 cm^2 active-area CCMs with three different Pt cathode loadings. Use of i_{eff} is important for proper analysis of the cathode kinetics at low current density where the cross-over current density approaches the measured current density. The data for each Pt cathode loading fall onto a straight line in this semi-logarithmic plot, with apparent Tafel-slopes of 0.063 V per decade (0.15 mg_{Pt}/cm^2), 0.066 V per decade (0.24 mg_{Pt}/cm^2), and 0.067 V per decade (0.4 mg_{Pt}/cm^2) over the entire current density range (0.02–1.8 A/cm^2). The Tafel-slopes extracted from Fig. 6a are consistent with the Tafel-slopes for the ORR in PEFCs reported in the literature (ranging from 0.053 to 0.064 V per decade [2,23–25]).

The following equation is generally applied to the analysis of fuel cell performance data and will be used to analyze the data in Fig. 6a:

$$\begin{aligned} E_{iR\text{-free}} &= E_{\text{cell}} + iR_{\Omega} \\ &= E_{\text{rev}(p_{H_2}, p_{O_2}, T)} - \eta_{\text{ORR}} - \eta_{\text{HOR}} - \eta_{\text{tx}} \end{aligned} \tag{3}$$

where $E_{\text{rev}(p_{H_2}, p_{O_2}, T)}$ is the temperature and partial pressure dependent equilibrium voltage, η_{ORR} and η_{HOR} the cathodic and anodic overpotential losses, and η_{tx} the diffusion overpotential losses. Based on the results in Section 3.1, it is quite reasonable to assume that the anode overpotential losses, η_{HOR}, are negligible, particularly for the high anode loadings (0.4 mg_{Pt}/cm^2) used in the MEAs shown in Fig. 6a. Assuming furthermore that diffusion overpotential losses are negligible for pure reactants, Eq. (3) can be reduced to

$$E_{iR\text{-free}} = E_{\text{rev}(p_{H_2}, p_{O_2}, T)} - \eta_{\text{ORR}} \tag{4}$$

Using a Tafel approximation, the last term in Eq. (4) can be described as

$$\eta_{\text{ORR}} = \text{TS} \log \left[\frac{i + i_x}{10 L_{\text{ca}} A_{\text{Pt,el}} i_{0(T, p_{O_2})}} \right] \tag{5}$$

where L_{ca} (mg_{Pt}/cm^2) is the Pt cathode loading, $A_{\text{Pt,el}}$ (m^2_{Pt}/g_{Pt}) the electrochemically available Pt surface area in the MEA (52 m^2_{Pt}/g_{Pt} in this case [5]), and $i_{0(T, p_{O_2})}$ the exchange-current density for the ORR which depends on temperature and oxygen partial pressure. Eqs. (4) and (5) may be combined and re-written as

$$\begin{aligned} E_{iR\text{-free}} = E_{\text{rev}(p_{H_2}, p_{O_2}, T)} &+ \text{TS} \log \left[10 A_{\text{Pt,el}} i_{0(T, p_{O_2})} \right] \\ &- \text{TS} \log \left[\frac{i + i_x}{L_{\text{ca}}} \right] \end{aligned} \tag{6}$$

Assuming that the utilized Pt surface area in the different CCMs, $A_{\text{Pt,el}}$, is essentially independent of the Pt loading (see [5]), Eq. (6) shows that the performance of the CCMs with different Pt cathode loadings is expected to be identical if it is plotted as $E_{iR\text{-free}}$ versus the logarithm of $(i + i_x)/L_{\text{ca}}$ (i.e. the mass-specific current density, i_m) and if the performance is controlled only by the ORR kinetics and the ohmic losses. The predicted slope of the resulting line should then correspond to the Tafel-slope

$$\begin{aligned} &\left. \frac{\partial E_{iR\text{-free}}}{\partial \log[i + (i_x/L_{\text{ca}})]} \right|_{p_{O_2}, p_{H_2}, T, A_{\text{Pt,el}}} \\ &= \left. \frac{\partial E_{iR\text{-free}}}{\partial \log[i_m]} \right|_{p_{O_2}, p_{H_2}, T, A_{\text{Pt,el}}} = -\text{TS} \end{aligned} \tag{7}$$

Replotting the data shown in Fig. 6a in terms of $E_{iR\text{-free}}$ versus the logarithm of the mass-specific current density, i_m, indeed results in a single straight line with a Tafel-slope of 0.065 mV per decade as shown in Fig. 6b, confirming that the measured ohmic resistance, R_{Ω}, and the ORR kinetics are the only terms which control the H_2/O_2 polarization curves shown in Fig. 6a. The exchange-current density evaluated from Fig. 6b and normalized to an O_2 partial pressure of 100 kPa is 6.7×10^{-9} A/cm^2_{Pt}, consistent with other data in the literature (see [5] for a detailed discussion).

Therefore, for *state-of-the-art* MEAs, resistance-corrected cell voltage losses at any given current density with respect

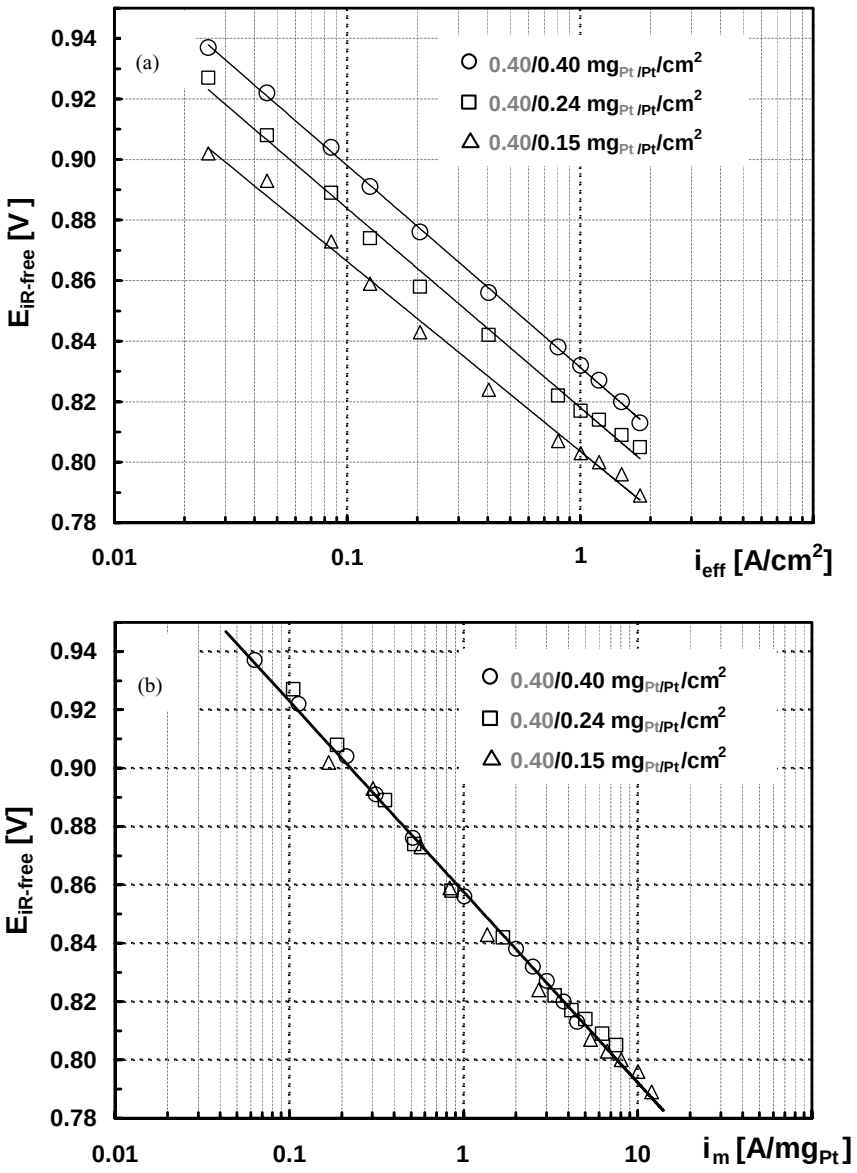

Fig. 6. Effect of cathode Pt loading on resistance-corrected single-cell voltage ($E_{iR\text{-free}}$), for H_2/O_2 operation vs.: (a) effective geometric current density (yielding Tafel-slopes of 0.067, 0.066, and 0.063 V per decade for cathode loadings of 0.40, 0.24, and 0.15 mg_{Pt}/cm^2, respectively) and (b) mass-specific current density (Tafel-slope of 0.065 V per decade). Test conditions: in-house prepared Nafion® 112 catalyst-coated membranes using 1100 EW ionomer in the electrodes and 47 wt.% Pt/carbon catalyst (0.40 mg_{Pt}/cm^2 cathode loadings), operated in 50 cm^2 single-cells at 80 °C and 270 kPa_{abs} with fully humidified reactants (80 °C dewpoints) at stoichiometric H_2/O_2 flows of 2.0/9.5 (in the entire range from 0.022 to 1.80 A/cm^2). Cell resistances were determined by on-line high-frequency resistance measurements (at 1 kHz) and the measured current densities were corrected for H_2 cross-over of 3.3 mA/cm^2 ($i_{eff} = i + 3.3\,mA/cm^2$) determined from voltammetric experiments. Voltages were averaged between 10 and 15 min holding time at each current density.

to changes in cathode loading can be described by

$$\left.\frac{\partial E_{iR\text{-free}}}{\partial \log[L_{ca}]}\right|_{p_{O_2}, p_{H_2}, T, A_{Pt,el}, i_{eff}} = -TS \quad (8)$$

predicting a loss of ca. 65 mV for a cathode loading reduction by a factor of 10.

3.3.2. Cell voltage losses for reduced cathode catalyst loadings for H_2/air

Contrary to the H_2/O_2 performance, additional current density dependent mass-transport resistances, η_{tx}, affect H_2/air polarization curves, amounting to ca. 50 mV at 1.0 A/cm^2 and >100 mV at 1.5 A/cm^2 (see [5]). In this case, an additional term must be added to Eq. (6):

$$E_{iR\text{-free}} = E_{rev(p_{H_2}, p_{O_2}, T)} + TS \log\left[10 A_{Pt,el} i_{0(T, p_{O_2})}\right] - TS \log\left[\frac{i + i_x}{L_{ca}}\right] - \eta_{tx} \quad (9)$$

Under these conditions, the prediction of the effect of the cathode loading, L_{ca}, on the resistance-corrected cell voltage, $E_{iR\text{-free}}$, is not straightforward anymore since the partial

derivative of Eq. (9) with respect to L_{ca} yields an expression in which the second term on the right-hand side is poorly defined:

$$\left.\frac{\partial E_{iR\text{-free}}}{\partial \log[L_{ca}]}\right|_{p_{O_2}, p_{H_2}, T, A_{Pt,el}, i_{eff}} = -TS - \left.\frac{\partial \eta_{tx}}{\partial \log[L_{ca}]}\right|_{p_{O_2}, p_{H_2}, T, A_{Pt,el}, i_{eff}} \quad (10)$$

If the observed mass-transport losses in H_2/air operation are related to either gas-diffusion resistances or to proton conduction resistances in the cathode structure, the derivative on the right-hand side of Eq. (10) will be non-zero and the resistance-corrected voltage loss upon reduction of the cathode catalyst loading cannot be predicted analytically. On the other hand, if the observed mass-transport losses with H_2/air are entirely due to gas-diffusion losses in the diffusion media, the derivative on the right-hand side of Eq. (10) should be zero and the resistance-corrected voltage losses upon reduction of the cathode catalyst loading can be predicted on the basis of Eq. (8), i.e. by purely considering the changes in the ORR kinetics.

In our previous study [5], a comparison of H_2/air and H_2/helox (helox: 21% O_2 in He) performance curves demonstrated that ca. 50% of the observed mass-transport related voltage losses were due to gas-diffusion resistances in the diffusion medium, whereas another 50% were likely to be due to proton transport resistances in non-optimized cathode structures. Therefore, for H_2/air operation with these MEAs one would expect voltage losses upon cathode catalyst reduction, which are different from purely kinetic losses.

Fig. 7 shows cell voltage differences between 500 cm^2 active-area MEAs with cathode loadings of 0.40 and 0.20 mg_{Pt}/cm^2 which were tested in a ca. 20-cell short-stack with H_2/air at 1.3/2.0 stoichiometric flows at 150 kPa_{abs} and 80 °C with partially humidified reactants (80/64 °C, dewpoints anode/cathode). The cell voltage loss, ΔE_{cell}, versus current density for the standard MEAs with "non-optimized cathode structure" (solid triangles) is between 30 and 50 mV, significantly larger than the purely kinetic voltage loss of 20 mV which can be calculated from Eq. (8) (i.e. 65 mV log[0.4/0.2]). As discussed above, this indicates the presence of either gas-diffusion resistances or proton conduction resistances in the cathode structure. Optimization of the cathode structure of these MEAs by a proprietary procedure which improves its proton conductivity, results in cell voltage losses of only 10–20 mV as the cathode catalyst loading is reduced by a factor of two (grey squares), consistent with purely ORR kinetics related losses (see Eq. (8)).

In summary, a reduction of the platinum cathode loading from 0.40 to 0.20 mg_{Pt}/cm^2 in *state-of-the-art* MEAs operated with H_2/air results in cell voltage losses of only 20 mV. Further cathode loading reductions would be expected to follow Eq. (8) and experiments are underway to prove this hypothesis.

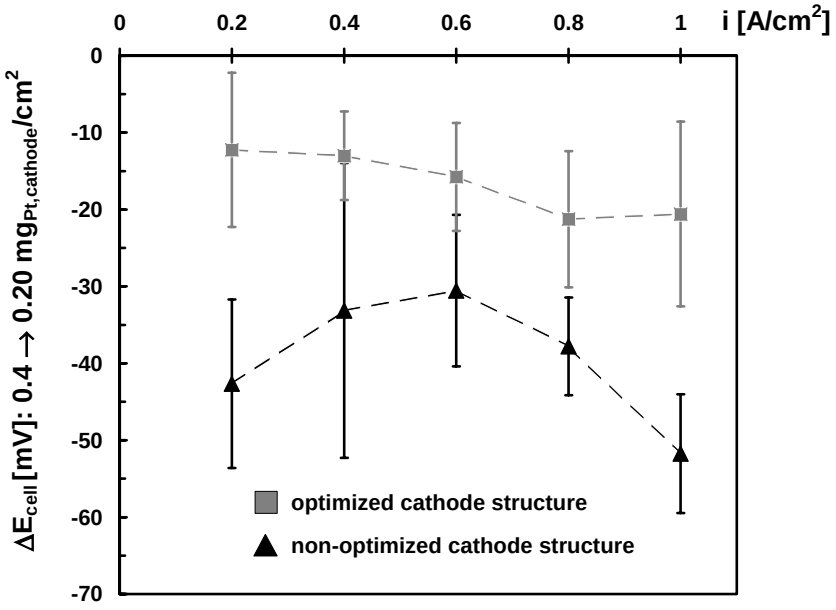

Fig. 7. Cell voltage losses, ΔE_{cell}, between 500 cm^2 active-area MEAs with reduced cathode loadings referenced to MEAs with cathode loadings of 0.40 mg_{Pt}/cm^2 (all anode loadings are 0.40 mg_{Pt}/cm^2). 500 cm^2 active-area MEAs were tested in a short-stack (four replicate MEAs for each loading) at 80 °C and 150 kPa_{abs} with partially humidified H_2/air (80/64 °C dewpoints anode/cathode) at stoichiometric flows of $s = 1.3/2.0$ (H_2/air). The "non-optimized cathode structure" CCMs (solid triangles) were prepared according to the same procedure and using the same components as the 50 cm^2 catalyst-coated membranes described in Fig. 2; "optimized cathode structure" CCMs (gray squares) were prepared according to an improved proprietary procedure which improves the proton conductivity in the cathode electrode structure but uses the same components (i.e. catalysts, ionomers, membranes). Voltages were averaged between 10 and 15 min holding time at each current density.

4. Conclusions

We have shown that anode Pt loadings in *state-of-the-art* MEAs operated with H_2/air can be reduced without significant voltage losses to 0.05 mg_{Pt}/cm^2, while cathode Pt loadings can be reduced to 0.20 mg_{Pt}/cm^2 with a voltage loss of only 20 mV up to 1.0 A/cm^2. Based on Fig. 2, this would result in a cell voltage of 0.63 V at 1.0 A/cm^2 (80 °C, 150 kPa_{abs}, stoichiometric flows of 2.0/2.0, reactant dewpoints of 80/64 °C) for Nafion® 112 based MEAs at a total loading of 0.25 mg_{Pt}/cm^2 per MEA, corresponding to 0.4 g_{Pt}/kW, a value which is very close to the automotive targets quoted in [13]. Further improvements in the Pt-specific power density are possible with thinner membranes and low-EW ionomers, which allow to obtain the same cell voltage at even higher current densities [5]. Beyond this, the implementation of Pt-alloy catalysts promises an additional reduction of Pt cathode loadings by a factor of two [2,14], reducing the Pt-specific power density well into the target range for large-scale automotive fuel cell applications with pure H_2 fuel.

On the other hand, significant R&D efforts are still required for the reduction of the Pt-metal-specific power density in reformate/air applications since the current *state-of-the-art* PtRu anode catalysts cannot be reduced to below 0.3 g_{PtRu}/kW for only the anode side, unless either CO-impurities in reformate can be reduced significantly below 100 ppm, the operating temperature can be increased to significantly above 80 °C, or more effective CO-tolerant catalysts are being developed.

Acknowledgements

We would like to acknowledge the contributions from Rohit Makharia who prepared and tested the Nafion® 112 based catalyst-coated membranes. Furthermore, we would like to thank Mike Scozzafava for preparing many of the MEAs used in this study. Last but not least, we would like to thank Mark Mathias and Bhaskar Sompalli for many fruitful discussions.

References

[1] S. Gottesfeld, T.A. Zawodzinski, in: R.C. Alkire, H. Gerischer, D.M. Kolb, C.W. Tobias (Eds.), Advances in Electrochemical Science and Engineering, vol. 5, Wiley, Weinheim, 1997, pp. 195–301.
[2] T.R. Ralph, M.P. Hogarth, Platinum Met. Rev. 46 (2002) 3.
[3] D.P. Wilkinson, A.E. Steck, in: O. Savadogo, P.R. Roberge (Eds.), Proceedings of the Second International Symposium on New Materials for Fuel Cell and Modern Battery Systems, Ecole Polytechnique de Montreal, Montreal, 1997, pp. 27–35.
[4] D.P. Wilkinson, J. St.-Pierre, PEM fuel cell durability, in: W. Vielstich, A. Lamm, H.A. Gasteiger (Eds.), Handbook of Fuel Cells: Fundamentals, Technology, and Applications, vol. 3, Chapter 47, Wiley, 2003, p. 611.
[5] H.A. Gasteiger, W. Gu, R. Makharia, M.F. Mathias, B. Sompalli, Beginning-of-life MEA performance–efficiency loss contributions, in: W. Vielstich, A. Lamm, H.A. Gasteiger (Eds.), Handbook of Fuel Cells: Fundamentals, Technology, and Applications, vol. 3, Chapter 46, Wiley, 2003, p. 593.
[6] M. Nakao, M. Yoshitake, Composite perfluorinated membranes for PEM fuel cells, in: W. Vielstich, A. Lamm, H.A. Gasteiger (Eds.), Handbook of Fuel Cells: Fundamentals, Technology, and Applications, vol. 3, Chapter 32, Wiley, 2003, p. 412.
[7] S. Cleghorn, J. Kolde, W. Liu, Catalyst Coated Composite Membranes in: W. Vielstich, A. Lamm, H.A. Gasteiger (Eds.), Handbook of Fuel Cells: Fundamentals, Technology, and Applications, vol. 3, Chapter 44, Wiley, 2003, p. 566.
[8] O.J. Murphy, G.D. Hitchens, D.J. Manko, J. Power Sources 47 (1994) 353.
[9] T.R. Ralph, G.A. Hards, J.E. Keating, S.A. Campbell, D.P. Wilkinson, M. Davis, J. St-Pierre, M.C. Johnson, J. Electrochem. Soc. 144 (1997) 3845.
[10] M.S. Wilson, S. Gottesfeld, J. Appl. Electrochem. 22 (1992) 1.
[11] S.S. Kocha, Principles of MEA preparation for PEM fuel cells, in: W. Vielstich, A. Lamm, H.A. Gasteiger (Eds.), Handbook of Fuel Cells: Fundamentals, Technology, and Applications, vol. 3, Chapter 43, Wiley, 2003, p. 538.
[12] D.J. Wheeler, J.S. Yi, R. Fredley, D. Yang, T. Patterson Jr., L. VanDine, J. New Mater. Electrochem. Syst. 4 (2001) 233.
[13] C. Jaffray, G. Hards, Precious metal supply requirements, in: W. Vielstich, A. Lamm, H.A. Gasteiger (Eds.), Handbook of Fuel Cells: Fundamentals, Technology, and Applications, vol. 3, Chapter 41, Wiley, 2003, p. 509.
[14] N.M. Markovic, T.J. Schmidt, V. Stamenkovic, P.N. Ross Jr., Fuel Cells 1 (2001) 105.
[15] N.M. Markovic, B.N. Grgur, P.N. Ross, J. Phys. Chem. B 101 (1997) 5405.
[16] L.W. Niedrach, D.W. McKee, J. Paynter, I.F. Danzig, Electrochem. Technol. 5 (1967) 318.
[17] S. Gottesfeld, J. Pafford, J. Electrochem. Soc. 135 (1988) 2651.
[18] T.R. Ralph, M.P. Hogarth, Platinum Met. Rev. 46 (2002) 117.
[19] K. Ruth, M. Vogt, R. Zuber, Development of CO-tolerant catalysts for PEMFCs, in: W. Vielstich, A. Lamm, H.A. Gasteiger (Eds.), Handbook of Fuel Cells: Fundamentals, Technology, and Applications, vol. 3, Chapter 39, Wiley, 2003, p. 489.
[20] M. Murthy, M. Esayian, A. Hobson, S. MacKenzie, W.-K. Lee, J.W. Van Zee, J. Electrochem. Soc. 148 (2001) A1141.
[21] R.J. Bellows, D.T. Buckley, E.P. Marucchi-Soos, in: J. McBreen, S. Mukerjee, S. Srinivasan (Eds.), Proceedings of the Symposium on Electrode Materials and Processes for Energy Conversion and Storage IV, The Electrochemical Society, PV 97-13, 1997, p. 1.
[22] T.J. Schmidt, H.A. Gasteiger, R.J. Behm, J. Electrochem. Soc. 146 (1999) 1296.
[23] S. Mukerjee, S. Srinivasan, J. Electroanal. Chem. 357 (1993) 201.
[24] S. Mukerjee, S. Srinivasan, A.J. Appleby, Electrochim. Acta 38 (1993) 1661.
[25] E.A. Ticianelli, C.R. Derouin, S. Srinivasan, J. Electroanal. Chem. 251 (1988) 275.